Available online at www.sciencedirect.com

ScienceDirect

Procedia Engineering 213 (2018) 730–742

Procedia Engineering

www.elsevier.com/locate/procedia

7th International Conference on Fatigue Design, Fatigue Design 2017, 29-30 November 2017, Senlis, France

Fatigue Life Prediction of Al319-T7 Subjected to Thermo-Mechanical Loading Conditions

Hong Tae Kang[a,*], Yung-Li Lee[b], Jim Chen[b], Xiao Wu[a]

[a]*The University of Michigan-Dearborn, 4901 Evergreen Road, Dearborn, MI4812, USA*
[b]*FCA USA LLC., 1000 Chrysler Dr., Auburn Hills, MI48326, USA*

Abstract

This study investigated a fatigue life prediction method based on extensive experiment results of cast aluminum alloy Al319-T7 subjected to repeated thermal and mechanical loading. Cyclic tests and fully reversed fatigue test results of the material were obtained from the specimens subjected to three different strain rates ($5x10^{-5}$, $5x10^{-4}$ and $5x10^{-3}$) and various temperature conditions. At each strain rate the specimens were subjected to room temperature (25°C), 150°C, 200°C, 250°C and 300°C. Thermo-mechanical fatigue (TMF) tests were also conducted for in-phase and out-of-phase conditions of the temperature and mechanical loading. During the thermo-mechanical fatigue tests, the effect of loading phases and dwell time on fatigue life of the specimens was also observed. This study modified Taira's fatigue damage model for thermo-mechanical loading condition to include the strain rate effect on the fatigue damage. Taira assumed that fatigue damage per reversal is proportional to the damage factor, $\lambda(T)$, and plastic strain range powered by n, $(\Delta\varepsilon_p)^n$. The relationship between the plastic strain range ($\Delta\varepsilon_p$) and the number of cycles to failure (N_f) is presented as $\lambda(T)\bullet(\Delta\varepsilon_p)^n\bullet N_f = C$. Where C is a temperature independent material constant. The temperature effect is included in the damage factor, $\lambda(T)$ that can be determined from the ratio of $\lambda(T)/\lambda(T_o)$ for low cycle fatigue test results at various isothermal conditions. T_o is the reference temperature and can be determined by experiment. This study used stress range applied instead of plastic strain range in the original equation. Furthermore, the modified equation includes the effect of strain rate, phase, and dwell time. The new fatigue damage equation was well correlated with the experiment results.

Peer-review under responsibility of the scientific committee of the 7th International Conference on Fatigue Design.

* Corresponding author. Tel.: +1-313-593-1878; fax: +1-313-593-5386.
E-mail address: htkang@umich.edu

1877-7058
Peer-review under responsibility of the scientific committee of the 7th International Conference on Fatigue Design.
10.1016/j.proeng.2018.02.069

Keywords: cast aluminum alloy; isothermal fatigue; thermomechanical fatigue; damage model; life prediction

1. Introduction

In automotive industry, the durability of engine components at high temperature is one of the major considerations in the design phase since they are usually running under the service environment of cyclic loading and high temperature. While most engine components were made of cast iron in the past, many cast iron components have been replaced by aluminum alloys nowadays to reduce the vehicle weight. Along with the use of light weight components in the vehicle, thermal loadings as up as to 300˚C can be applied to engine components [1]. With the strong demand to understand the thermos-mechanical behavior of aluminum alloy engine parts and predict their service life, many efforts have been made in the past decades.

Thomas et al. [2] proposed a complete design approach and lifetime prediction method for aluminum alloy cylinder heads under thermos-mechanical fatigue (TMF) loading. Engler-Pinto et al. [3] investigated the thermos-mechanical fatigue behavior of cast 319 aluminum alloys used in cylinder blocks. Kang et al. [4] introduced a fatigue life prediction method for thermo-mechanical fatigue damage under variable temperature and loading amplitudes using a rainflow cycle counting technique. Wei et al. [5, 6] reviewed the up-to-date methods for damage modelling and life assessment of components under thermal fatigue loading and developed a general life assessment procedure under variable amplitude thermal-mechanical loadings, emphasizing on hold-time effect. Santacreu et al. [7-9] proposed a TMF damage model of stainless steels based on the maximal temperature and plastic strain amplitude reached during a thermal cycle.

This study reviewed Taira's damage model [10] for thermal fatigue first. Then A modification was made on Taira's damage model by using stress amplitude range instead of plastic strain range. Isothermal fatigue tests were used to validate its ability for correlating the data from different temperatures and different strain rates. And the model was further modified to analysis TMF loading cases, which includes in-phase (IP) and out-of-phase (OP) tests with dwell time and without dwell time, respectively. Finally, the TMF test results were found to be well correlated with the proposed new fatigue damage equation. All the necessary tests were conducted and the test results were reported in [11].

2. Taira's Damage Model

Taira [10] assumed that fatigue damage per reversal is proportional to the damage factor, $\lambda(T)$, and plastic strain range powered by n, $(\Delta\varepsilon_p)^n$. The relationship between the plastic strain range ($\Delta\varepsilon_p$) and the number of cycles to failure (N_f) is presented as below:

$$\lambda(T) \bullet (\Delta\varepsilon_p)^n \bullet N_f = C \tag{1}$$

where C is a temperature independent material constant and n is the material exponent, which is taken as 2 in most cases. The temperature effect is included in the damage factor, $\lambda(T)$ that can be determined from the ratio of $\lambda(T)/\lambda(T_o)$ for low cycle fatigue test results at various isothermal conditions. T_o is the reference temperature. Figure 1 shows an example for a carbon steel and a stainless steel.

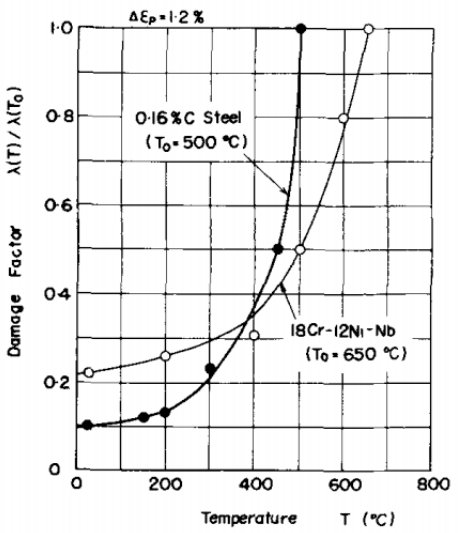

Fig. 1. Temperature dependence on the damage factor λ(T) [10].

For elevated temperature case an equivalent temperature (T_e) was obtained from two different ways that depend on the temperature range. If the cyclic temperature range ($\Delta T = T_2 - T_1$) is in lower temperature range, the equivalent temperature is simply the mean temperature of T_1 and T_2. When the cyclic temperature is close to or within the high-temperature level, T_2 becomes the equivalent temperature. The schematic diagram in Figure 2 presents the relationship between damage factor $\lambda(T_e)$ and the equivalent temperature (T_e).

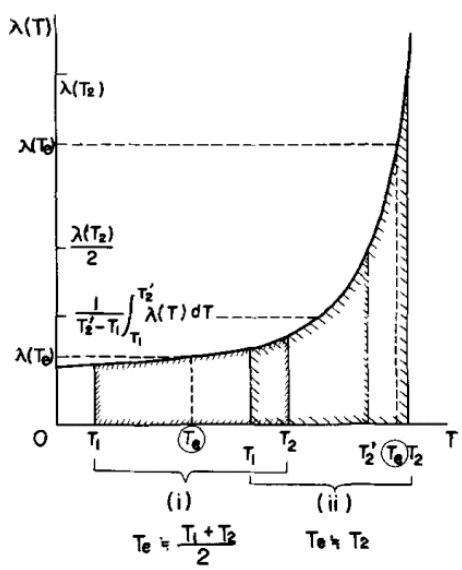

Fig. 2. Schematic representation of the relation between $\lambda(T_e)$ and T_e [10].

Santacreu and co-workers [7] employed Taira's damage model [10] to predict the fatigue life of stainless sheet steels subjected to thermo-mechanical loading. The modified Taira's damage model is presented below [7]:

$$N = \lambda\left(T_{eq}\right)\Delta\varepsilon_p^t \tag{2}$$

Where, λ is function of an equivalent temperature, T_{eq}, and t is independent of temperature. The equivalent temperature is defined as below:

$$T_{eq} = \frac{T_{\max}}{1 - aT_{\max}\left[\ln(1 + b\tau)\right]} \tag{3}$$

Where, τ is the dwell time, a and b are parameters obtained from experiments.

3. Modification of Taira's Damage Model

Current study planned to employ the modified Taira's damage model as shown in Equations (1) and (2). However, the plastic strain range was not sensitive to represent the fatigue damage of AL319-T3 material as shown in Figure 3. Instead stress range at a stabilized cycle showed better correlation with the fatigue life of AL319-T7 specimens as shown in Figure 4. Thus, the Taira's damage model is modified to accommodate this change in this study.

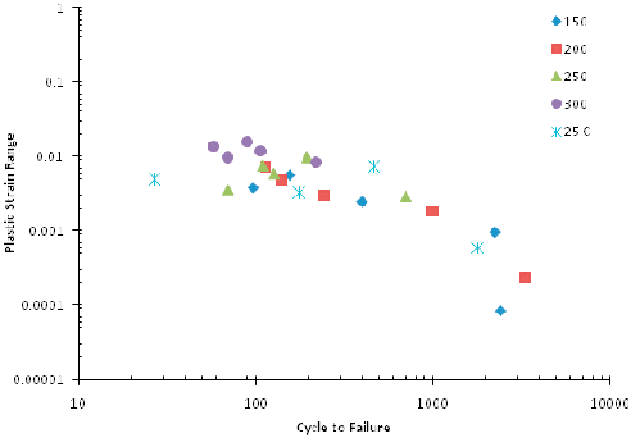

Fig. 3. Plastic strain range versus cycles to failure at various temperatures.

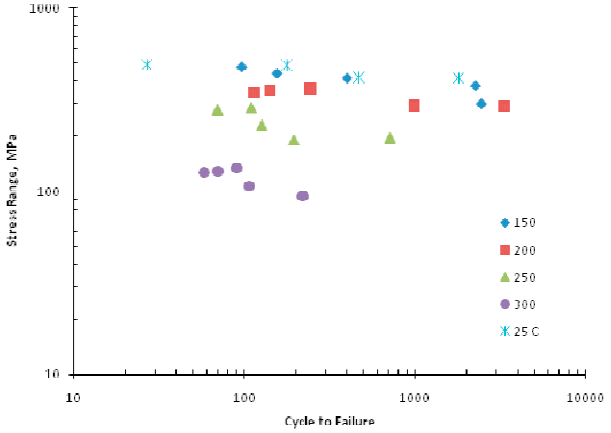

Fig. 4. Stress range versus cycles to failure at various temperatures.

Thus, the Equation (1) is modified in this study as below:

$$\lambda_1(T) \bullet \lambda_2(\dot{\varepsilon}) \bullet (\frac{\Delta\sigma}{2}) \bullet N_f = C \quad (4)$$

Where $\lambda_1(T)$ is damage factor due to temperature and $\lambda_2(\dot{\varepsilon})$ is damage factor due to strain rate. First the damage factor due to temperature at each strain rate is determined by the ratio of stress amplitude at the current temperature and the reference temperature at the same cycle. The reference temperature is 300°C in this study. The damage factor due to temperature is presented in Figure 5 for the strain rate of $5x10^{-5}$. The scatter at each temperature is caused from the scatter of damage factor at the cycle where it is evaluated. The fitted curve represents the damage factor due to temperature at strain rate of $5x10^{-5}$. By incorporating this damage factor to the stress amplitude versus cycles to failure curve, Figure 6 is obtained. For each strain rate the similar relationship is developed for the damage factor due to temperature as shown in Figure 7. As shown in the figure, strain rate effect is observed on the fatigue life of the AL319-T7 even if the same stress amplitude is applied. Thus, the damage factor for the strain rate is developed as shown in Figure 8. As observed in the thermal fatigue testing data, more damage was observed at the lower strain rate testing. Thus, the lowest strain rate, $5x10^{-5}$, becomes the reference strain rate for the damage factor curve of the strain rate effect. Stress amplitude after incorporating the damage factors due to temperature and strain rate effect is plotted with cycles to failure of the specimens tested in Figure 9. The developed modified Taira's damage model is presented with fatigue test results at different temperatures and strain rates in Figure 10. As shown in the figure the test results are reasonably well correlated to the modified equation of Taira's damage model.

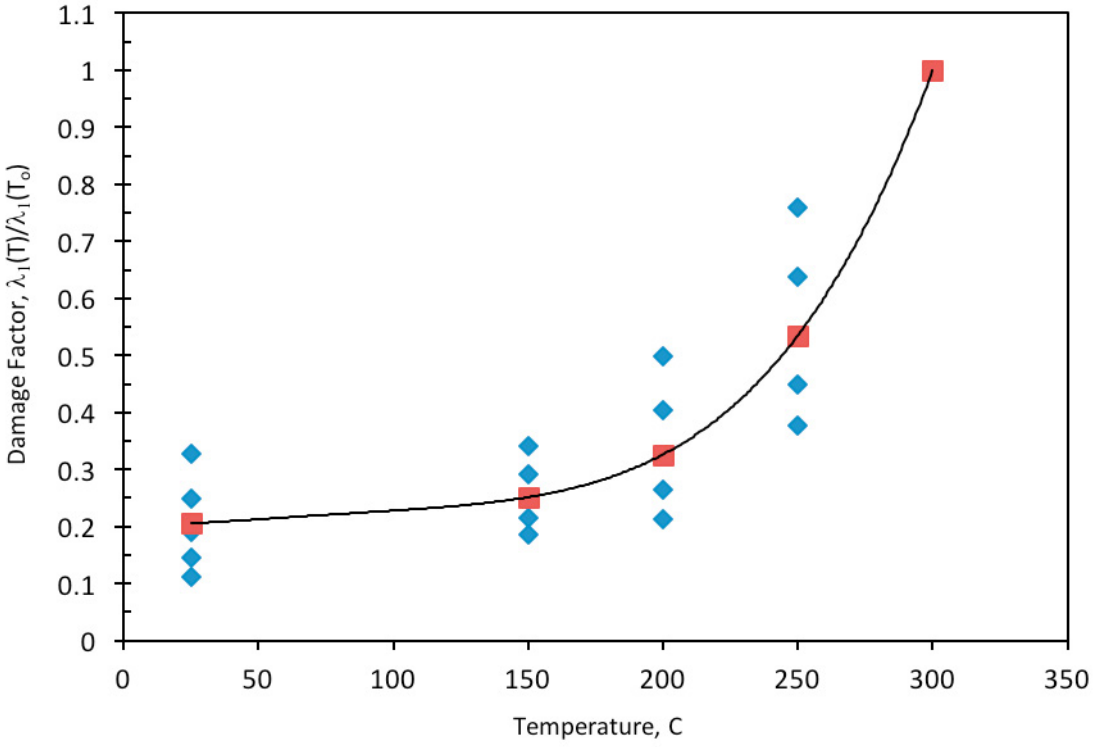

Fig. 5. Damage factor for different temperatures at the strain rate of $5x10^{-5}$.

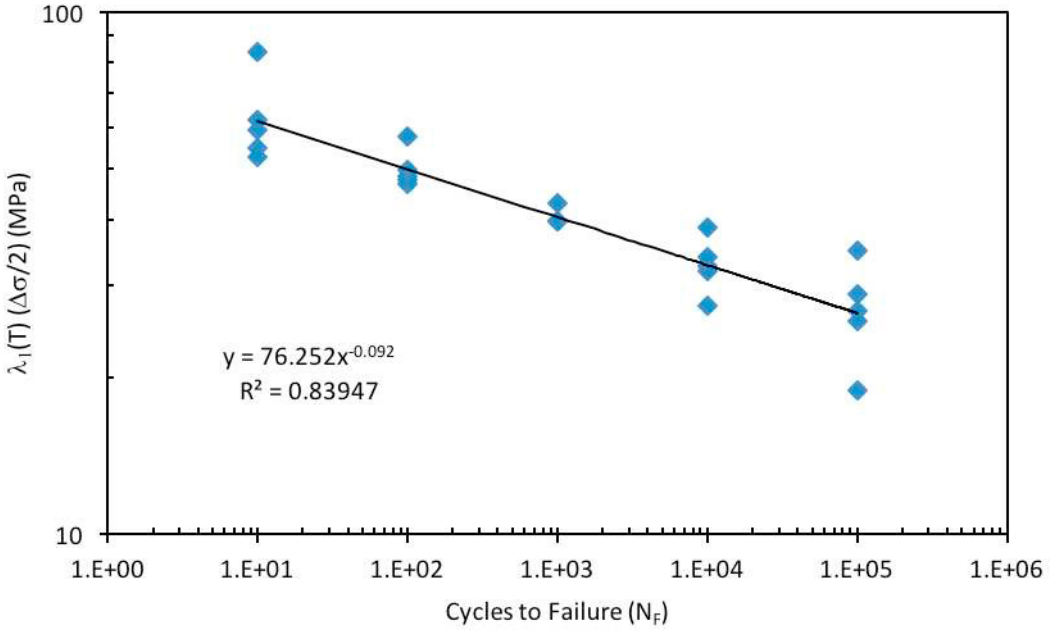

Fig. 6. Stress amplitude versus cycles to failure after incorporating the damage factor.

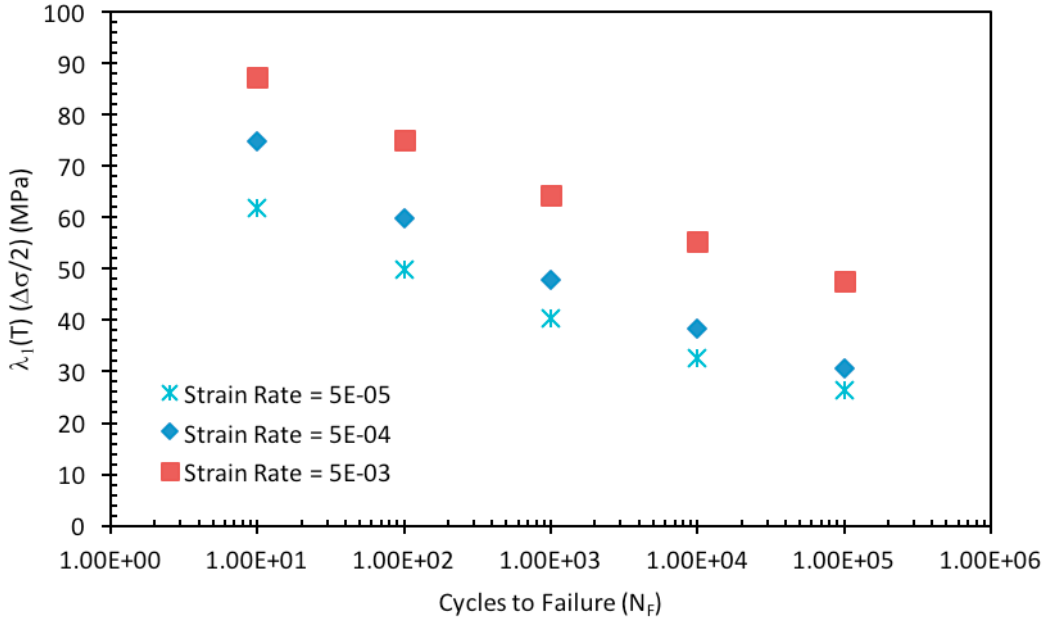

Fig. 7. Strain rate effect after incorporating damage factor due to temperature.

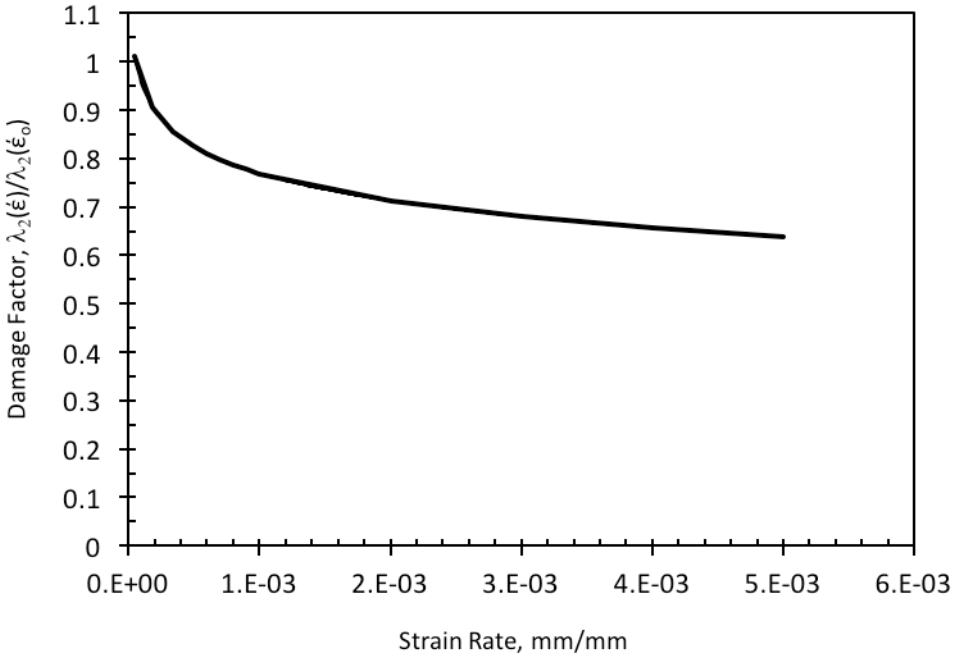

Fig. 8. Damage factor curve due to strain rate effect.

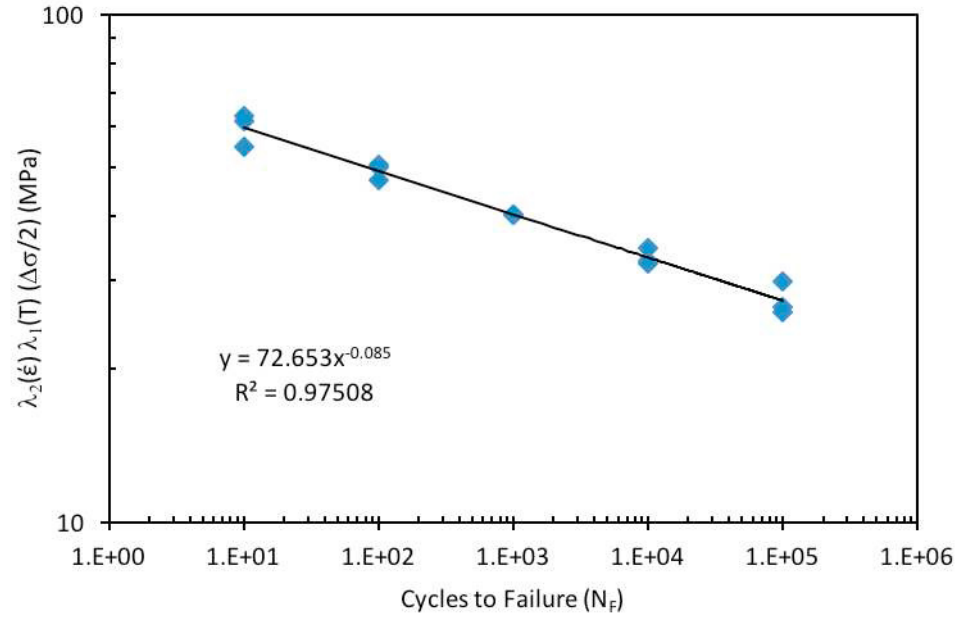

Fig. 9. Stress amplitude versus cycles to failure after incorporating the damage factors due to temperature and strain rate.

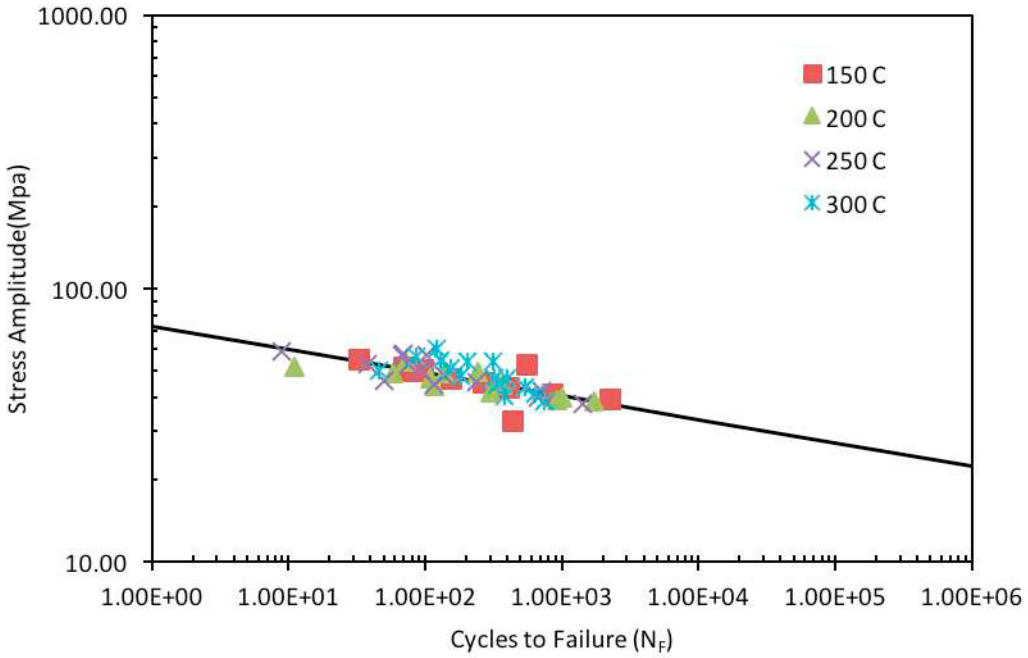

Fig. 10. Test data with the curve developed from modified Taira's damage model.

4. Modified Taira's Damage Model for TMF

The isothermal fatigue test results at various temperatures and strain rates were presented with the modified Taira's model using stress amplitude at the stabilized cycle. Now, the modified Taira's model is further developed to be used for thermo-mechanical fatigue loading cases. This study considered in-phase with dwell time (IP-WD), in-phase without dwell time (IP-WOD). out-of-phase with dwell time (OP-WD), and out-of-phase without dwell time (OP-WOD) for TMF loading cases.

To employ the modified Taira's model for TMF loadings, temperature (equivalent temperature, T_{eq}) equivalent to the isothermal temperature should be determined for the TMF loading case. Santacreu and co-workers [7] used the equivalent temperature equation as shown in Equation (3). Basically, Equation (3) presents that the equivalent temperature is equal to the maximum temperature when no dwell time is applied. If dwell time is included in TMF loading, Equation (3) needs two parameters (a and b) to obtain the equivalent temperature. However, it is not clear how a and b are obtained but mentioned those were obtained from test results. This study tried to use the same equation but it was identified the limitation of the equation. For example, the equation does not explicitly define the phase effect on the determination of the equivalent temperature.

Thus, this study used a different equation to determine the equivalent temperatures for various TMF loading conditions as shown below:

$$T_{eq} = T_{max}(1-\alpha+\beta X) \tag{5}$$

where T_{max} is the maximum temperature of the TMF loading, α is phase effect (=0.125 for OP and =0.0833 for IP), and β is the dwell time effect (=0.04163). X is either 1 with dwell time or zero without dwell time.

Once the equivalent temperature (T_{eq}) is determined, the damage factor due to the equivalent temperature, $\lambda_1(T_{eq})$, and strain rate, $\lambda_2(\dot{\varepsilon})$, are determined as explained in the modified Taira's model. The relationship between the equivalent temperature and fatigue life is expressed as below:

$$\lambda_1(T_{eq})\lambda_2(\dot{\varepsilon})\frac{\Delta\sigma}{2} = C(N)^d \tag{6}$$

where C is the coefficient and d is the exponent, which are determined from test data. Then, the damage factor due to phase effect or dwell time effect needs to be multiplied to the left hand side of the Equation (6). As mentioned earlier, this study considered the in-phase and the out-of-phase of temperature and mechanical loading with dwell time and without dwell time for each phase. The test results for the IP-WOD and OP-WOD from this study and from a literature are plotted as shown in Figure 11. The slopes of IP and OP are found to be almost the same value.

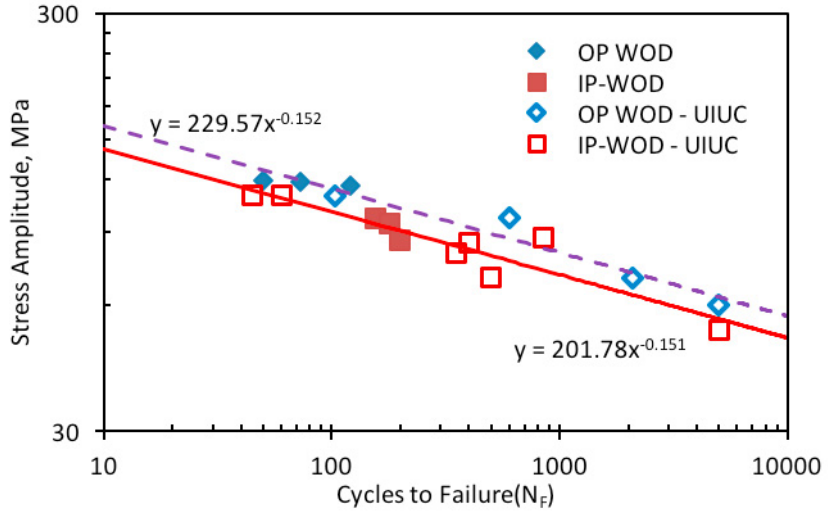

Fig. 11. Stress amplitude versus cycles to failure for IP-WOD and OP-WOD.

The test results for IP-WD and OP-WD are very limited from this study and no other literatures are reported for AL319-T7. Thus, it is assumed that the slope of the curve for IP-WD and IP-WOD is the same, and the same assumption is applied to OP-WD and OP-WOD. Without these assumptions, the obtained test data may lead to the wrong conclusion because of the limited data. Figure 12 shows the stress amplitude versus cycles to failure for IP-WD and OP-WD.

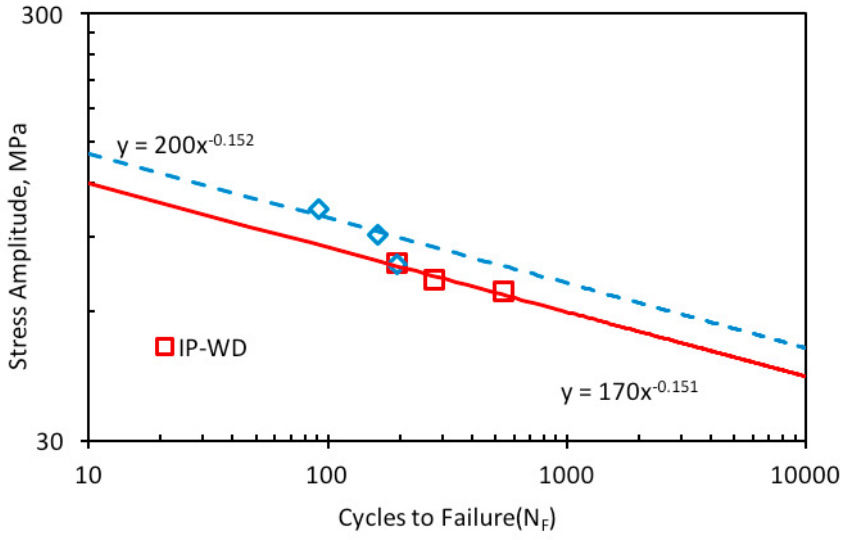

Fig. 12. Stress amplitude versus cycles to failure for IP-WD and OP-WD.

However, the slopes obtained from isothermal fatigue test results and those obtained from TMF are different as shown in Figure 13. Thus, it is necessary to introduce a damage factor representing each curve of TMF test. Figure 14 represents the generalized curve (representing for T_{eq}) and four curves for TMF conditions after applying the damage factor to the gerneralized curve. As seen in Figure 14, the damage factor is a function of fatigue life. Thus one more step is necessary to obtain the final euqtion to represent the relationship between stress amplitude and fatigue life under TMF loading conditions. Figue 15 shows a damage factor representaion in fuction of fatigue life.

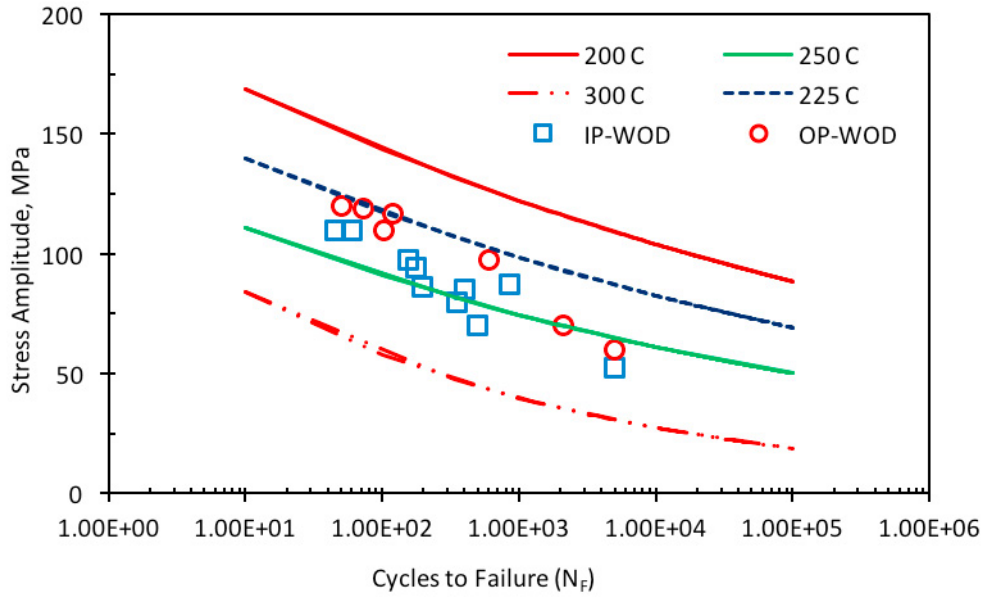

Fig. 13. Isothermal and TMF test results.

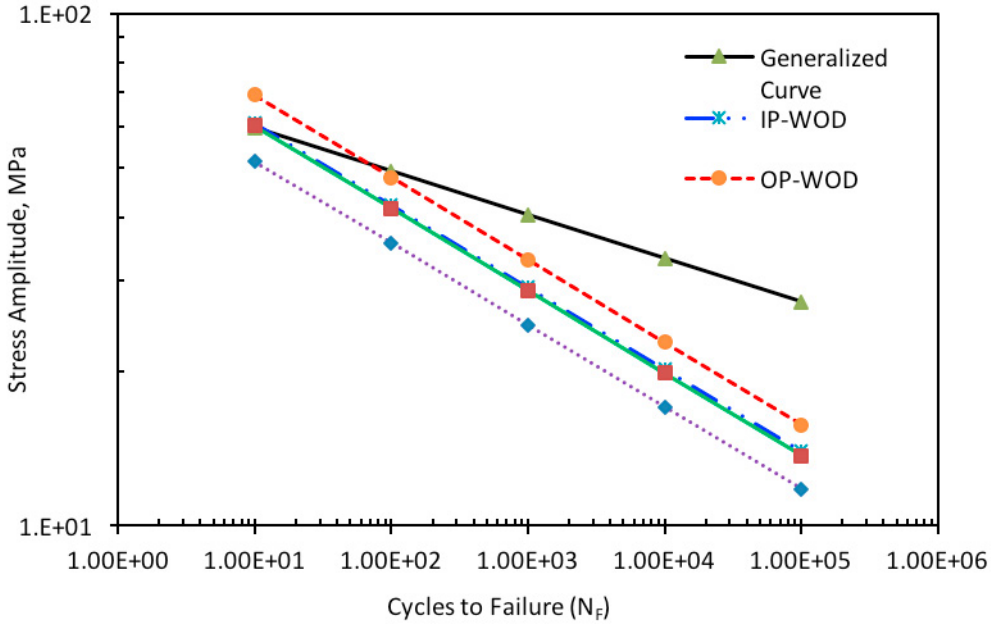

Fig. 14. Generalized curve and TMF curves.

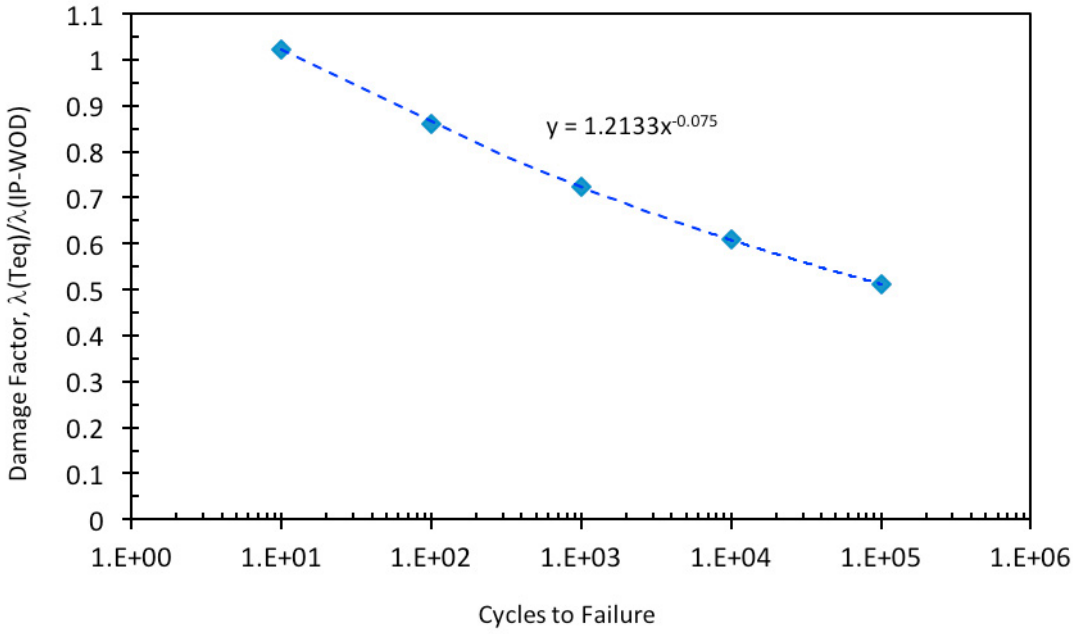

Fig. 15. damage factor representation for IP-WOD.

The damage factor for TMF is determined by the stress amplitude ratio at the given fatigue life. Then, the damage factor is multiflied to the left had side of the Equation (6). Thus the Equation now becomes:

$$\lambda_1(T_{eq})\lambda_2(\dot{\varepsilon})\lambda_3(\eta)\frac{\Delta\sigma}{2} = F(N)^g \tag{7}$$

where $\lambda_3(\eta)$ is the damage factor due to a TMF loading condition.

Therefore, now fatigue life (N) can be calculated for any TMF loading conditions using above equation. Here is an example procedure how to use the Equation (7) due to the damage factor for IP-WOD:

A. Calculate stress amplitude ratios between IP-WOD and *Teq* at cycles to failure at every increament of 10, 100, 1,000, 10,000, and 100,000.
B. Then, obtain the best-fit curve equation by plotting the stress ratio versus cycles to failue.
C. From the Equation (6) obtain N corresponding to $(\frac{\Delta\sigma}{2})$ and determine the damage factor for IP-WOD using the best-fit curve equation obtained from the step B.
D. Finally use the Equation (7) to calculate the fatigue life (N) of IP-WOD.

Figure 16 shows the comparison of the prediction curves for all the TMF loading cases and the test results. It can be found that the test results are well correlated with the prediciton curves determined from Eq. (7), which is modified from the equation dedicated to the isothermal fatigue tests. And the modified Taira's equation is able to include the effect of temperature, strain rate, loading phase, and dwell time.

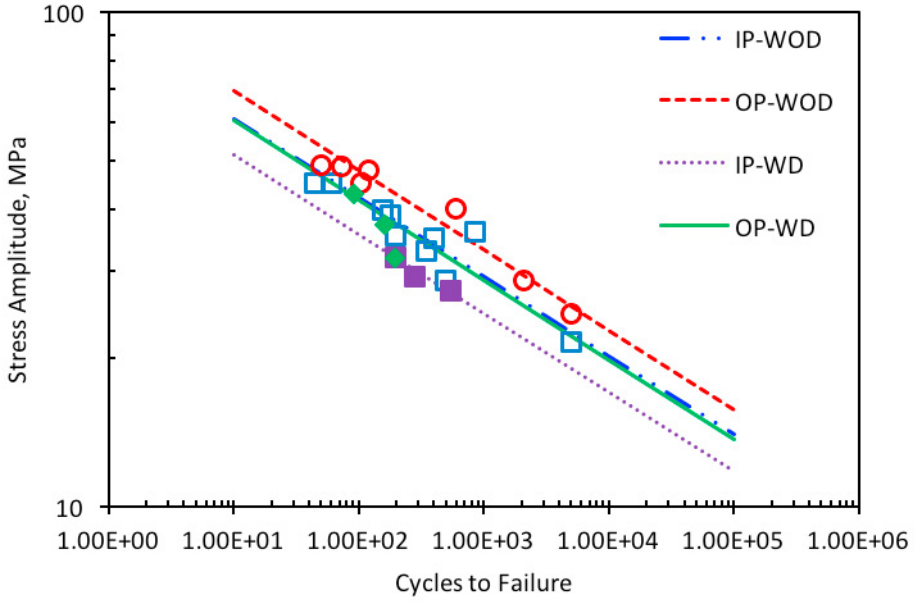

Fig. 16. TMF test data with the curves developed from modified Taira's damage model.

5. Conclusion

Based on Taira's damage model for thermal fatigue, this paper modifies it by using the stress amplitude range instead of plastic strain range, since the stress amplitude is found to be more suitable in order to distinguish the effect of temperature on aluminum alloy Al319-T7 invesitaged here. Isothermal fatigue tests are first analyzed using this modified damage model, in which temperature effect and strain rate effect are considered by adding two coressponding damage factors. These damage factors can be determined from the experimenal tests using the procedure described in the paper. The proposed damage model are found to be reasonably correlated with the test data under different testing temperatures and various strain rates.

And the proposed damage model is then further applied on TMF loading cases, by incorporating another damage factor to consider the loading phase effect happened in the TMF data. In-phase (IP) and out-of-phase (OP) loading tests, with and without dwell time, have been analyzed in this work. And isothermal fatigue data are used to help generate the additional damage factor. With the new damage factor included, the TMF test results are well presented with the proposed new fatigue damage model. The future work will be using finite element analysis tool to validate the proposed approach on real components under isothermal conditions.

Acknowledgements

References

[1] T.J. Smith, H. Sehitoglu, E. Fleury, H.J. Maier, J. Allison, Modeling high-temperature stress-strain behavior of cast aluminum alloys, Metallurgical and Materials Transactions A, 30 (1999) 133-146.

[2] J.-J. Thomas, L. Verger, A. Bignonnet, E. Charkaluk, Thermomechanical design in the automotive industry, Fatigue & Fracture of Engineering Materials & Structures, 27 (2004) 887-895.

[3] C. Engler-Pinto, H. Sehitoglu, H. Maier, T. Foglesong, Thermo-mechanical fatigue behavior of cast 319 aluminum alloys, European Structural Integrity Society, 29 (2002) 3-13.
[4] H.T. Kang, Y.-L. Lee, J. Chen, D. Fan, A thermo-mechanical fatigue damage model for variable temperature and loading amplitude conditions, International Journal of Fatigue, 29 (2007) 1797-1802.
[5] Z. Wei, S. Lin, L. Luo, F. Yang, D. Konson, A Thermal-Fatigue Life Assessment Procedure for Components under Combined Temperature and Load Cycling, in, SAE Technical Paper, 2013.
[6] Z. Wei, L. Luo, B. Lin, F. Yang, D. Konson, K. Ellinghaus, M. Pieszkalla, K. Avery, J. Pan, C.C. Engler-Pinto, Hold-Time Effect on Thermo-Mechanical Fatigue Life and its Implications in Durability Analysis of Components and Systems, Materials Performance and Characterization, 4 (2014) 198-217.
[7] P. Santacreu, H. Sassoulas, F. Moser, O. Cleizergues, G. Lovato, Study of the thermal fatigue of stainless steels and its application to the life prediction of automotive exhaust line components, in: Thermal Stresses'99: Third International Congress on Thermal Stresses, 1999, pp. 245-248.
[8] P.-O. Santacreu, L. Bucher, A. Koster, L. Rémy, Thermomechanical fatigue of stainless steels for automotive exhaust systems, Revue de Métallurgie, 103 (2006) 37-42.
[9] P.-O. Santacreu, L. Faivre, A. Acher, Damage Mechanisms of Stainless Steels under Thermal Fatigue, SAE International Journal of Materials and Manufacturing, 7 (2014) 553-559.
[10] S. Taira, Relationship between thermal fatigue and low-cycle fatigue at elevated temperature, ASTM STP, 520 (1973) 80-101.
[11] H.T. Kang, Effect of Temperature and Strain Rate on Material Characteristics of Al319-T7, Procedia Engineering, (2017), submitted